 

# New scintillators for fast and thermal neutron detection

*N.Z.Galunov, N.L.Karavaeva, V.P.Seminozhenko*[*]

Institute for Scintillation Materials, STC "Institute for Single Crystals", National Academy of Sciences of Ukraine, 60 Lenin Ave., 61001 Kharkiv, Ukraine
[*]State Scientific Institution "Institute for Single Crystals", National Academy of Sciences of Ukraine, 60 Lenin Ave., 61001 Kharkiv, Ukraine

*Received March 6, 2012*

Proposed a technology to obtain a new class of detectors, namely organic composite scintillators. It allows us to create the scintillation detectors of an unlimited area. We consider hydrogen-bearing composite scintillators as the detectors of fast neutrons. The composite scintillators based on gadolinium silicate and pyrosilicate are discussed as the thermal neutron detectors. As well we consider the combined detector for selective detection of thermal and fast neutrons in the presence of background gamma radiation. Scintillation characteristics of the composite detectors are analyzed in comparison with the scintillation systems based on single crystals.

Предложена технология получения нового класса детекторов — органических композиционных сцинтилляторов. Предложенная технология позволяет создавать детектирующую систему неограниченной площади. Рассмотрены водородосодержащие композиционные сцинтилляторы как детекторы быстрых нейтронов. В качестве детекторов тепловых нейтронов обсуждаются композиционные сцинтилляторы на основе силиката и пиросиликата гадолиния. Рассматривается комбинированный детектор для селективной регистрации тепловых и быстрых нейтронов в присутствии фонового гамма-излучения. Сцинтилляционные характеристики композиционных детекторов анализируются в сравнении с традиционными монокристаллическими системами.

## 1. Introduction

The problem of spectrometry of low intensity fluxes of fast neutrons and alpha particles is of a great importance in modern ecological, geological, biological, medical fields, custom survey, etc. Such radiations are among the most hazardous for human organism. The hazard is characterized by the radiation-weighting factor. The radiation-weighting factor $W_R$ is the value expressing the long-term risk (primarily cancer, leukemia, heavy pulmonary allergies, etc.) of a low-level chronic exposure. It depends on a radiation type and other factors. For example, for gamma radiation photons $w_R = 1$, while for fast neutrons with energy $E_n < 2$ MeV, the $w_R = 20$. Similar high $w_R$ values characterize alpha particles. For thermal neutrons, $w_R = 5$ [1]. In the natural conditions there are numerous hydrogen-contain media in which the fast neutrons are moderated very fast and become the thermal neutrons. The detection of such the thermal neutrons only allows the estimation of the flux of primary fast neutrons. To detect a very low activity of ionizing radiations, large size detectors are necessary. In such a case the increase of detection efficiency is attained due to the growth of spatial angle of detection. In the same time, such detectors should provide the spectral composition of luminescence making it possible to use the commercial (and thus inexpensive) photodetectors. The materials should provide the separate detection of neutrons and background gamma radiation, and show a sufficiently high light yield.

In this work we describe two preparation procedures of composite scintillators for (i) fast neutrons basing on grains of stilbene and *p*-terphenyl crystals and (ii) thermal neutrons basing on grains of gadolinium silicate $Ce{:}Gd_2SiO_5$ (Ce:GSO) and pyrosilicate $Ce{:}Gd_2Si_2O_7$ (Ce:GPS). This work is relevant, because the maximum size of the organic scintillation single crystals grown from the melt is 150 mm and that of gadolinium pyrosilicate single crystals, tens of the millimeters. The Ce:GSO single crystals were first proposed for detection of thermal neutrons in [2], and Ce:GPS single crystals, in [3].

We proposed and studied as well a new composite scintillation detector. It is a combined detector for (iii) separate detection of fast neutrons and thermal neutrons in the presence of gamma background radiation.

## 2. Technologies

The grains of different size can be obtained when a single crystal is crushed or ground. To choose the necessary fraction of the grain sizes the calibrated sieves with different cell sizes were used [4]. In the cases under discussion the linear size $L$ of organic grains varied from 0.5 up to 4.5 mm and inorganic grains, from 0.06 up to 1.0 mm. The crystalline grains were added into a two-component polymer matrix. The prepared composite material was placed into an optically transparent organic glass container [4, 5].

### 2.1. Composite scintillators for fast neutron detection

The fast neutrons generate in the organic material the recoil protons with maximum energy equal to that of neutrons. The grain size should be at least equal to the recoil proton path in the grain material. Therefore, depending on the energy of neutrons to be detected, the scintillators have to be prepared basing on fractions of various sizes (from submillimeter range to several millimetres). The technology included the following stages [4–7].

– The purification of raw material that includes the oriented crystallization process.

– Preparation of grains and separation thereof into fractions of different sizes.

– Preparation of organosilicone polymeric dielectric gel.

– Introduction of the grains of a chosen fraction into the gel matrix to prepare the sample.

– The sample introduction into the shaping container.

– Evacuation and holding of the sample during 48 hours.

– Application of the reflective coating onto the container.

As the polymer matrix, the two-component dielectric gel Sylgard-527 (Dow Corning Corporation, USA) was used due to its inertness, non-hygroscopicity, and maximum transparency in the stilbene luminescence range. It should be noted that the technique we used does not require growing of single crystals with high structural perfection [5–7]. Really, as the result of the oriented crystallization process we obtain the material consisting of the single crystal grains which have random orientations. After the process of crystal growth we obtain the boule, which has perfect crystal structure. When we douse the crystalline material in liquid nitrogen, it cracks along the crystal structure defects. The first experiments have shown that the optimum amount of stilbene grains in the immersion medium is at least 70 % of the matrix mass [5]. The scintillator height should provide an efficient detection of fast neutrons of several MeV and the scintillator must remain sufficiently transparent to its intrinsic emission. The container was been made of organic glass. These processing methods have been used to prepare large-diameter ($\varnothing 200$ mm $\times$ 20 mm) composite detector based on stilbene grains and doped *p*-terphenyl grains.

### 2.2. Composite scintillators for thermal neutron detection

The inorganic detector thickness should be sufficient to detect thermal neutrons and the secondary radiations generated by those. On the other hand, the same detector should be thin enough to reduce probability of detecting background gamma-radiation. For such thin scintillator (but not limited in diameter), the efficiency of thermal neutron detection will exceed that of background radiations.

To prepare the crystal grains, Ce:GSO and Ce:GPS crystals were mechanically ground. Thus, the Ce concentration in the grains was the same as in the reference single crystals [8]. The grains were sieved through calibrated sieves to obtain the grains with necessary size $L_{GSO}$ and $L_{GPS}$. The grains of the chosen fractions were introduced into non-luminescent Sylgard-527 silicone material. Then the composition was

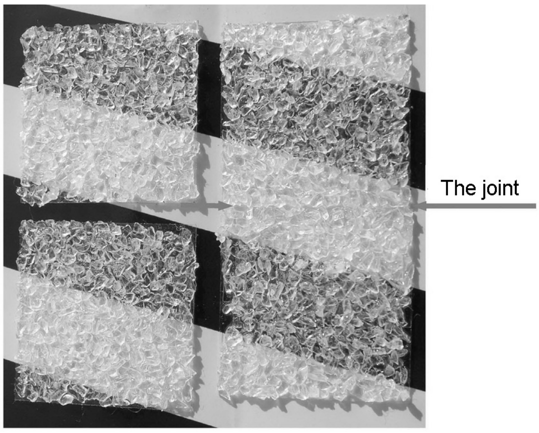


Fig. 1. Obtaining of the uniform piece of a composite scintillation material from the primary separate composite scintillators.

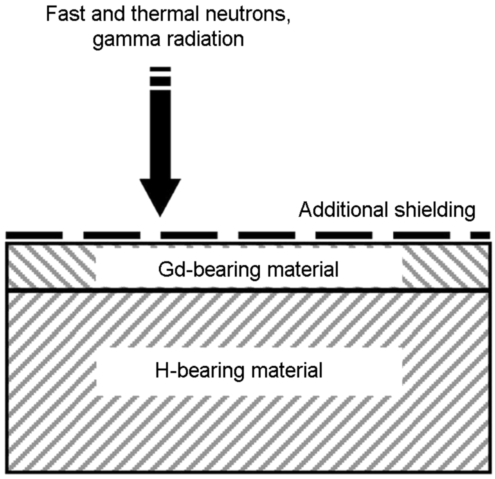


Fig. 2. Schematic diagram of a combined composite detector, which consists of a H-bearing fast neutron detector and a Gd-bearing thermal neutron detector.

applied onto an optically transparent non-luminescent organic glass plate [9, 10].

To study further the single-layer composite scintillators on the base of Ce:GSO and Ce:GPS grains, 5 grain size ranges (fractions) with $L_{GSO}$- or $L_{GPS}$-values, namely, less than 0.06, from 0.06 to 0.1, from 0.1 to 0.3, from 0.3 to 0.5, and from 0.5 to 1 mm. Additionally, grains with $L_{GSO}$ from 0.5 to 1.0 mm was used to prepare multi-layer (3 or 5 layers) Ce:GSO composite scintillators.

Technology of preparation of a composite material does not limit the area or shape of scintillation detector input window [10, 11]. Really, we can use a small amount of the gel to band two separate pieces of a composite scintillator together and to obtain the uniform piece of a scintillation material, which is the composite scintillator with the same scintillation properties as the primary separate composite scintillators (see Fig. 1).

### *2.3. Combined detectors*

Fig. 2 schematically shows a sandwich design of a combined composite detector. It consists of two different combined composite scintillation materials.

The lower scintillation material is based on stilbene crystalline grains. This part of the combined composite scintillator detects fast neutrons. As it was shown in [11–13] such a composite scintillator has the same pulse shape discrimination ability as the single crystal that was used to obtain the grains. A thin composite detector of thermal neutrons (the upper rectangle on Fig. 2) contains Ce:GPS or Ce:GSO crystalline grains introduced in the same matrix as in the previous case. As it was shown [9] for such the composite scintillator based on Ce:GPS or Ce:GSO crystalline grains with average sizes $L_{av} \leq 0.5$ mm, the efficiency of detection of gamma radiations with energies higher than 150 keV is negligible in comparison with the efficiency of thermal neutrons detection.

Fig. 3 shows the photographs of the combined detectors. The combined detectors were 30 mm in diameter. The composite scintillator (1) is a single-layer scintillator. To make it we used Ce:GPS (or Ce:GSO) crystalline grains. Mainly we used 3 fractions of grains with average sizes from 0.06 to 0.1, from 0.1 to 0.3 and from 0.3 to 0.5 mm. It allows us to detect thermal neutrons with minimal gamma background [9]. The composite scintillator (2) was 20 mm high. To make it we used stilbene crystalline grains with sizes $L_S$ from 2.5 to 3.0 mm. The stilbene single crystal (3) had the same dimensions (30 mm in diameter and 20 mm high). Both scintillators (i.e. detects the thermal and fast neutrons) are mounted inside a cylindrical plastic cell. The scintillators were separated by additional plastic plate 2 mm thick.

## 3. Experimental

The signals from a 9954A Electron Tubes Ltd. photomultiplier tube [14] were applied to electronics. The signal from anode is applied to pulse shape discrimination cycles. The signal from next to the last dynode is used for amplitude analysis [15].

In the measurements we used radionuclide $^{239}$Pu–Be source of fast neutrons and photons of gamma-radiation. To obtain ther-

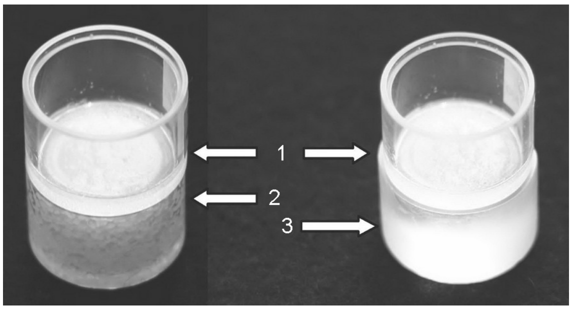


Fig. 3. The photographs of the combined composite detectors. The combined detector consists of two parts (see Fig. 2). There are a composite detector on the base of Ce:GPS (or Ce:GSO) grains (*1*) and a composite detector on the base of stilbene grains (*2*) or a stilbene single crystal (*3*).

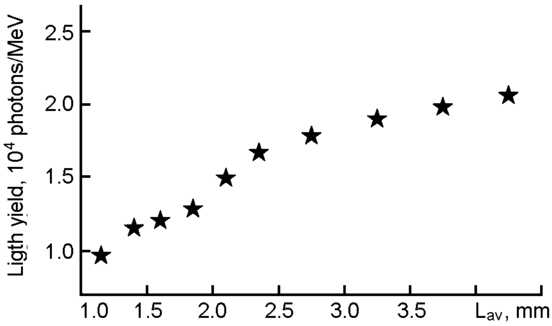


Fig. 4. Light yield of doped *p*-terphenyl composite scintillators with different grain size irradiated with 0.662 MeV photons of gamma radiation.

mal neutrons the source of fast neutrons was placed inside the calibrated paraffin sphere. We run the measurements with the $^{239}$Pu–Be radionuclide source that irradiates $1.0\cdot10^5$ fast neutrons per second or $9\cdot10^3$ thermal neutrons per second when it is mounted inside the calibrated paraffin sphere. If the flux of fast neutrons is $F_{fast}$ then $\eta_{th}\times F_{fast}$ thermal neutrons have to be irradiated in $4\pi$-geometry from the paraffin sphere. Therefore the $\eta_{th}$-value is taken as 0.09. The other neutrons, which permeate through the calibrated paraffin sphere, have the energies higher than the thermal energy.

We used a lead plate 20 mm thick to reduce the direct flux of low energy photons of gamma radiation from the neutron source. A thin (1.3 mm) cadmium plate prevented the flux of thermal neutrons to irradiate Gd-bearing scintillators. The difference in neutron fluxes measured with and without the cadmium plate allowed us to identify the events of thermal neutron detection.

In the measurements with fast neutrons the pulse shape discrimination technique was used to separate the fast neutron scintillations from the gamma background ones [15]. The procedure of the reconstruction a neutron spectrum from a corresponding recoil proton spectrum has been discussed in [16].

To calibrate the energy scale we used a set of gamma lines with the following energies $E_\gamma$: 17.0 keV ($^{241}$Am), 32.7 keV ($^{137}$Cs), 41 keV ($^{152}$Eu), 59.6 keV ($^{241}$Am), 77.9 keV ($^{152}$Eu), 122.0 keV ($^{152}$Eu). The light output of the scintillators relative to gamma energy $E_\gamma$ was linear to within 5 %. To calibrate the scale we used a calibrated reference stilbene single crystal with a low absolute light yield (12,000 photons/MeV) [8, 11].

The measurements of scintillation pulse shape were run according to the delayed-coincidence technique (see [17]). Gamma radiation from a $^{152}$Eu radionuclide source was used to measure the decay time $\tau$ of thin Gd-bearing detectors. To study a radioluminescence pulse shape of stilbene detectors we used $^{137}$Cs radionuclide source of gamma-radiation and $^{239}$Pu radionuclide source of alpha particles.

## 4. Results and discussion

### 4.1. Organic composite detectors

We investigated a series of 10 composite stilbene scintillators (∅30 mm × 20 mm) obtained from stilbene grains of different fractions, and analogous series of 10 composite scintillators based on *p*-terphenyl grains doped with 0.1 % of 1,4-diphenyl-1,3-butadiene.

The calculated values of light yield for a series of composite scintillators based on doped *p*-terphenyl grains excited with photons of gamma-radiation from $^{137}$Cs radionuclide source and alpha particles from $^{239}$Pu one, are presented in Figs. 4 and 5, respectively. For the gamma-radiation measurements (Fig. 4) the light yield values are given in absolute units. For the short-range alpha radiation (Fig. 5) these data are presented in percent; the light yield of standard doped *p*-terphenyl single crystal being taken as 100 %. The average values of the *p*-terphenyl grain size $L_p$ are given for each fraction of the grains. Figs. 4 and 5 show that the light yield reaches its maximum at $L_p$ ~ 2.5 mm and practically does not change with further increase of the average grain size value.

Fig. 6 presents a reconstructed neutron spectrum of the source $^{239}$Pu–Be for the composite *p*-terphenyl scintillator with the grain size fraction from 1.7 to 2.0 mm. In

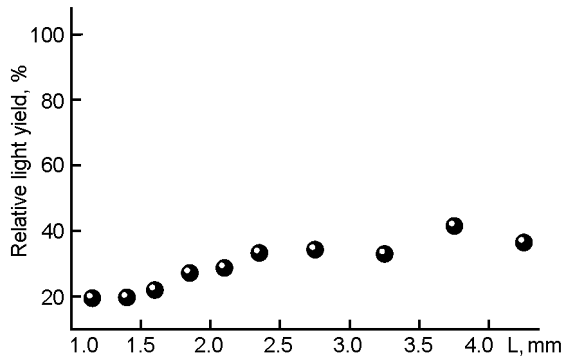


Fig. 5. Light yield of doped $p$-terphenyl composite scintillators with different grain size irradiated with 4.97 MeV alpha particles.

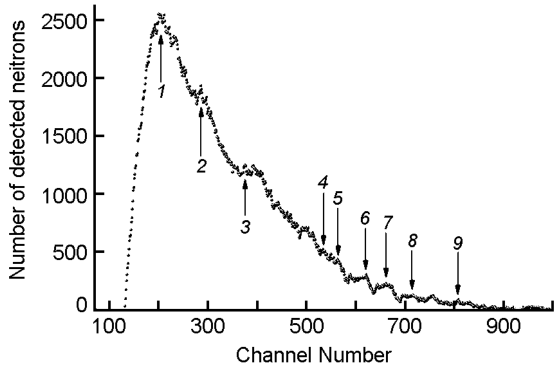


Fig. 6. Reconstructed neutron spectrum of $^{239}$Pu–Be source for a ∅30 mm×20 mm composite doped $p$-terphenyl scintillator with grain size $L_p$ ranging from 1.7 to 2.0 mm.

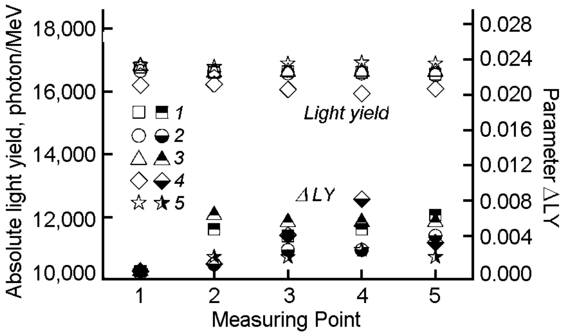


Fig. 7. Absolute light yield values measured at the points 1–5 for a series of ∅200 mm × 20 mm composite stilbene scintillators (the upper family of opened symbols) and the corresponding calculated values of $\Delta LY$ parameter (1) (the lower family of half-closed symbols).

this figure only are denoted only those fast neutron energies which are reported in theoretical and experimental papers for $^{239}$Pu–Be sources before (see the references in [16]), i.e. namely: 3.1, 4.2, 4.9, 6.4, 6.7, 7.3, 7.9, 8.6 and 9.7 MeV energies are denoted by the lines 1–9, respectively.

To estimate the degree of light yield non-uniformity we run the measurements with large-diameter (∅200 mm×20 mm) stilbene composite scintillators. We measured the light yield values by irradiating different parts of the scintillators, in particular, their centers and four additional zones. The latter were located on four mutually opposite sides of the scintillator, the distance between the centers of the scintillator and of any of the additional zone was 70 mm. The light yield values were measured according to the standard procedure using the source $^{137}$Cs. We characterized the degree of light yield non-uniformity by the parameter $\Delta LY$:

$$\Delta LY = \left| \frac{J_1 - J_i}{J_1 + J_i} \right|, \qquad (1)$$

where $J_1$ and $J_i$ were the light yield values measured at the scintillator center and at a point $i$, respectively. For $i = 1$ the value of $\Delta LY$ was taking as 1.

Fig. 7 presents the results of light yield measurements and the calculated values of the parameter $\Delta LY$ for 5 ∅200 mm × 20 mm composite scintillators obtained from crystalline stilbene grains. In Fig. 7 the dotted line shows the absolute light yield value for standard stilbene single crystal. The opened symbols correspond to the calculated values of light yield at the points of measurement; the half-closed ones are the calculated values of the parameter $\Delta LY$.

Analysis of these data testifies that the maximum spread of the light yield values measured for different parts of the large-diameter scintillators does not exceed the standard error of the method of light yield measurement (5 %). Thus, it should be concluded that the proposed technique gives reproducible results and allows us to make the homogeneous large-diameter composite detectors.

### 4.2. Inorganic composite detectors

As a result of thermal neutron capture, gadolinium radiates conversion electrons, characteristic X-ray and gamma radiation. When the influence of the edge effect is low the gadolinium-based scintillators have to show a characteristic 33 keV peak and along with it, a 77 keV peak that is the sum of the conversion electron peak (33 keV) and

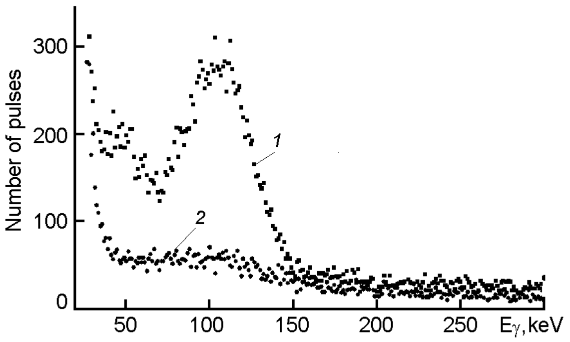


Fig. 8. The amplitude spectra of a 0.35 mm thick Cs:GPS single crystal were obtained without (curve *1*) and with (curve *2*) Cd-screen.

X-ray radiation (44 keV) [3]. The thickness of single-layer composite scintillators was determined as the average size of the corresponding fraction of grains, and for three-layer and five-layer Ce:GSO composite scintillators, as triple and fivefold value of the average fraction size includes $L_{\rm GSO}$ from 0.5 to 1 mm (i.e. 0.75 mm).

Figs. 8 and 9 demonstrate the results of the of the thermal neutron scintillation spectrum measurements by an example of Cs:GPS single crystal. Curve *1* in Fig. 8 is the scintillation spectrum of a Cs:GPS single crystal obtained as the result of irradiation by of all energies obtained after moderating fast neutrons from a $^{239}$Pu–Be source placed inside a paraffin sphere. Curve *2* represents the scintillation spectrum measured for the same experimental geometry but with the cadmium screen placed between the source and the scintillator. In this case the thermal neutrons are absorbed in the cadmium screen. The accumulation time was the same for both the spectra. The spectrum presented in Fig. 9 is obtained by subtraction of the curve *2* (Fig. 8) from the total scintillation spectrum that is presented by curve *1* in Fig. 8.

Fig. 10 shows the scintillation amplitude spectrum that was generated by thermal neutrons in a single-layer Ce:GPS composite scintillator (fraction of grains with grain size $L_{\rm GPS}$ from 0.3 to 0.5 mm). The obtained results have shown that the intensity ratio of 33 keV and 77 keV scintillation peaks increases as the grain size of a composite scintillator is diminished. The best neutron-to-gamma ratio was obtained for the single-layer composite scintillators. For Ce:GSO composite scintillators with 3 or 5 layers of 0.5–1 mm grains, the peak of 33 keV was not observed. For composite scintillators, the resolution of both lines is worse than for the reference single crystal. To characterize the properties of the scintillators, we have introduced three arbitrary energy ranges (see Fig. 10), namely, 20 to 55 keV (the amplitude range of the scintillation peak generated by 33 keV conversion electrons), 55 to 120 keV (the range of total 77 keV peak), and 20 to 120 keV (the whole scintillation spectrum).

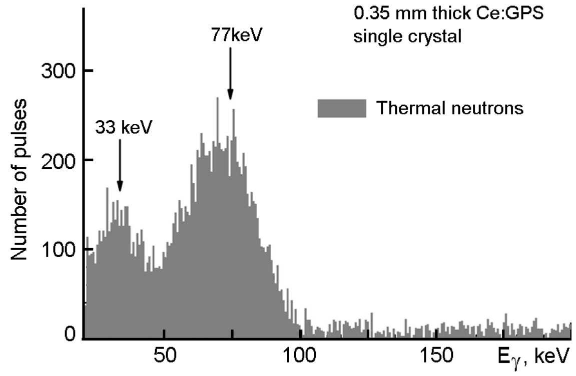


Fig. 9. The amplitude scintillation spectrum which is generated by thermal neutrons in a 0.35 mm thick Ce:GPS single crystal.

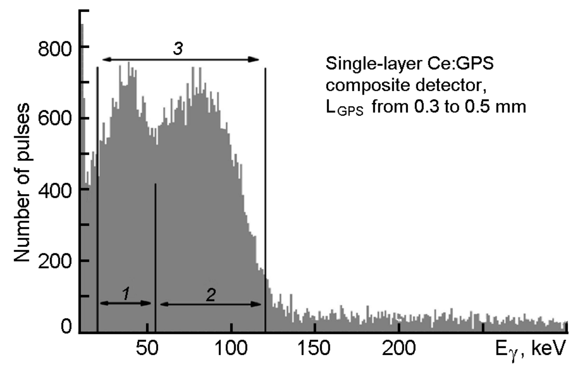


Fig. 10. The amplitude spectrum of a single-layer Ce:GPS composite detector with grain size $L_{\rm GPS}$ from 0.3 to 0.5 mm, which is excited by thermal neutrons.

### *4.3. Combined detectors*

#### *4.3.1. Decay time measurements*

Firstly, we analyzed a possibility to separate the scintillation signals obtained as the result of detection of the fast neutrons and thermal neutrons. Thereto we studied a scintillation pulse shape for corresponding scintillation materials of the combined detector.

Figs. 11 demonstrates the scintillation pulse shape for a single-layer composite scintillators based on grains of Ce:GPS with $L_{GPS}$ from 0.06 to 0.1 mm. Table 1 summarizes the results of measurements of the decay time constant τ for Gd-bearing detec-

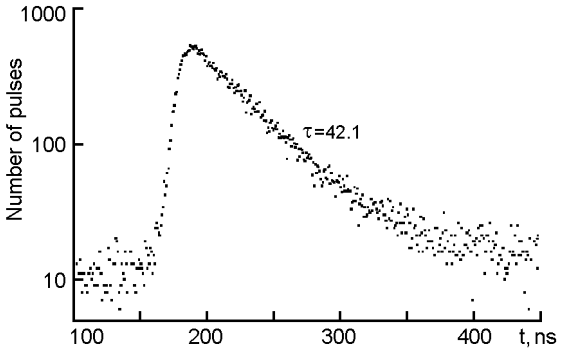


Fig. 11. The scintillation pulse shape of a single-layer Ce:GPS composite detector irradiated by photons of gamma-radiation of $^{152}$Eu.

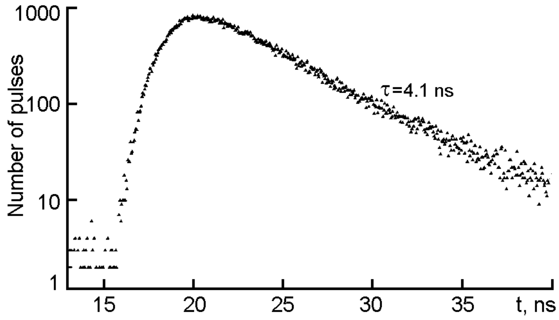


Fig. 12. The scintillation pulse shape of a stilbene single crystal irradiated by gamma photons of $^{137}$Cs.

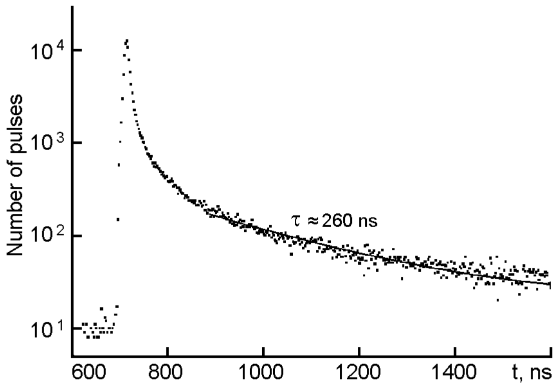


Fig. 13. The scintillation pulse shape of a stilbene single crystal irradiated by alpha particles of $^{239}$Pu. Squares present experimental data; solid line is their single-exponential approximation with a decay time constant τ.

tors. Some difference between τ-values obtained for the single crystals and for the corresponding composite detectors may be caused by inhomogeneous distribution of Ce in the reference crystal and in the grains used for obtaining the composite detectors [2, 3, 8].

For organic scintillators a scintillation pulse shape consists of two components. A fast component of the scintillation pulse is formed in the regions of low activation density (photons of gamma radiation, electrons). An ionizing particle with high specific energy losses (i.e. recoil protons generated by fast neutrons, alpha particle, etc.) forms the regions of high activation density. The energy exchange in these regions causes formation of the slow component of the scintillation pulse [17].

Fig. 12 and 13 demonstrate the scintillation pulse shape for a stilbene single crystal irradiated, correspondingly, by photons of gamma-radiation irradiated by $^{137}$Cs source and alpha particles of $^{239}$Pu source. They are practically the same for a single crystal and a composite scintillator and are the following. The decay time constant τ of the fast component of the scintillation pulse (Fig. 12) is about 4 ns, and a rough approximation of the slow component of the scintillation pulse shape by an exponent gives $\tau \approx 3 \cdot 10^2$ ns (see Fig. 13).

Decay time constants τ for scintillators based on Ce:GSO and Ce:GPS grains are about few tens of nanoseconds (Fig. 11, Table). This time is longer than τ-value of the scintillation pulse fast component and shorter than τ-value of the scintillation pulse slow component of organic scintillation materials. Therefore the standard approach [17], when a

Table. Decay time constant τ of Gd-bearing detectors

| Detector | τ, ns |
|---|---|
| Ce:GSO single crystal, thickness 0.39 mm (0.5 mol.% Ce) | 33.0 |
| Single-layer composite detector, Ce:GSO, $L_{GSO}$ from 0.06 to 0.1 mm | 44.5 |
| Single-layer composite detector, Ce:GSO, $L_{GSO}$ from 0.3 to 0.5 mm | 44.5 |
| Ce:GPS single crystal, thickness 0.35 mm (7 mol.% Ce) | 45.2 |
| Single-layer composite detector, Ce:GPS, $L_{GPS}$ from 0.06 to 0.1 mm | 42.1 |
| Single-layer composite detector, Ce:GPS, $L_{GPS}$ from 0.3 to 0.5 mm | 42.1 |

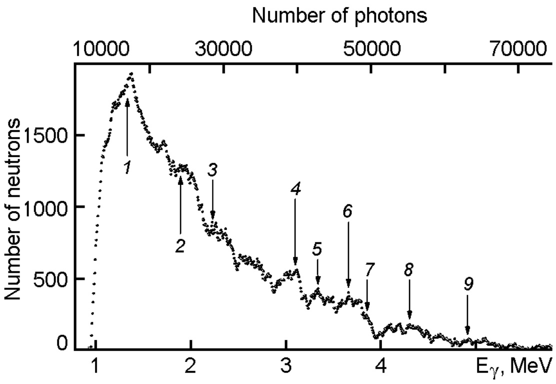


Fig. 14. The reconstructed neutron spectrum of the $^{239}$Pu–Be source obtained for the combined detector (a stilbene composite scintillator with $L_S$ from 2.5 to 3.0 mm and a Ce:GPS composite scintillator with $L_{GPS}$ from 0.06 to 0.1 mm).

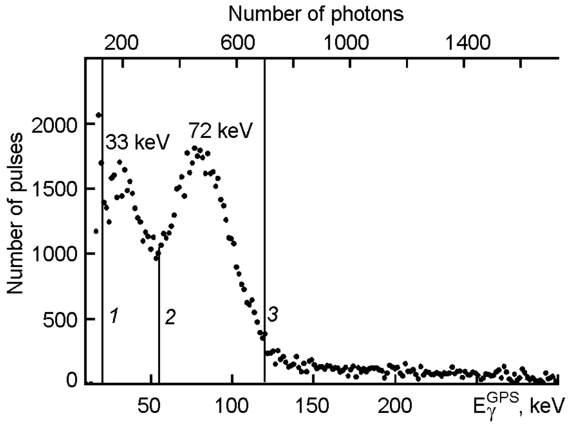


Fig. 15. A scintillation amplitude spectrum of the combined detector (a stilbene composite scintillator with $L_S$ from 2.5 to 3.0 mm and a Ce:GPS composite scintillator with $L_{GPS}$ from 0.06 to 0.1 mm) that was excited by thermal neutrons.

"short" time signal and a "long" time signal mean that it is the signals from different scintillation materials of a combined detector, seems not to be a good solution for the case under consideration. In this case another approach is required to separate the signals from different scintillation materials.

*4.3.2. Amplitude spectra measurements*

Fig. 14 shows the reconstructed neutron spectrum of the $^{239}$Pu–Be source measured by the combined detectors which consist of a stilbene composite detector with grain size $L_S$ and a Ce:GPS composite detector with grain size $L_{GPS}$. Peaks those are numbered from 1 to 9 correspond to the energies of neutrons 3.1, 4.2, 4.9, 6.4, 6.7, 7.3, 7.9, 8.6, and 9.7 MeV (see the references in [16]).

The bottom X-axis in Fig. 14 is presented as gamma equivalent. The values shown by the bottom X-axis in Fig. 14 are obtained as the value of the energy of gamma-radiation $E_\gamma$ which is necessary to obtain the scintillation pulse with the same amplitude (number of scintillation photons, see top X-axis) as for excitation of the scintillator by fast neutrons (see reconstructed neutron spectrum in Fig. 14). The energy scale (X-axis) was calibrated in scintillation photons i.e. in terms of a light yield by the reference calibrated stilbene single crystal. It gives the correlation between values of the bottom and the top X-axis. The neutron measurements were run after that and for the same measuring conditions.

Fig. 15 demonstrates the spectrum of thermal neutrons for the combined detector that contains a stilbene composite scintillator with $L_S$ from 2.5 to 3.0 mm and the Ce:GPS composite scintillator with $L_{GPS}$ from 0.06 to 0.1 mm. The bottom X-axis is calibrated in terms of scintillation amplitudes of a Ce:GPS composite scintillator that was excited by gamma-radiation with energies $E_\gamma^{GPS}$. The top X-axis is calibrated in terms of the number of scintillation photons. The solid lines 1, 2 and 3 show the energy ranges in which the signals from thermal neutrons were studied, i.e. around the peaks of 33 keV, 77 keV and the total signal for the both peaks.

Let $N_\Sigma$ be the number of events of thermal neutron detection, $t$ be the time of accumulation of these events, $F_{fast}$ be the fast neutron flux ($1 \cdot 10^5$ neutrons per second), $\eta_{th}$ be the number of thermal neutrons obtained by the moderation of fast neutrons in the paraffin sphere per one fast neutron (0.09), $S$ be the thermal neutron detector area, $R$ be the distance between the source and the detector. In such a case the efficiency of thermal neutron detection $\varepsilon_{th}$ can be estimated as follows [9]:

$$\varepsilon_{th} = \frac{N_\Sigma}{t \cdot F_{fast} \cdot \eta_{th} \cdot \dfrac{S}{4\pi R^2}}. \qquad (2)$$

Fig. 16 presents the results obtained according to (2). It shows the efficiency of thermal neutron detection $\varepsilon_{th}$ for a series of combined detectors with different $L_{GPS}$ and $L_S$ from 2.5 to 3.0 mm. The thickness is taken as average value of $L_{GPS}$ for a given fraction of grains. The calculations were made for three energy ranges, namely, from

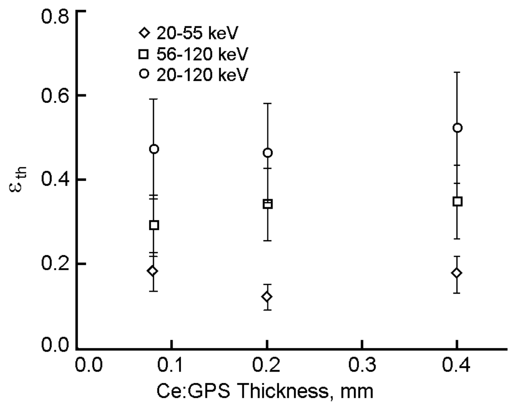


Fig. 16. The $\varepsilon_{th}$-values for the combined detectors (a stilbene composite scintillator with $L_S$ from 2.5 to 3.0 mm and a Ce:GPS composite scintillator with different $L_{GPS}$) those were obtained for different energy ranges of the scintillation amplitude spectrum (see Fig. 15).

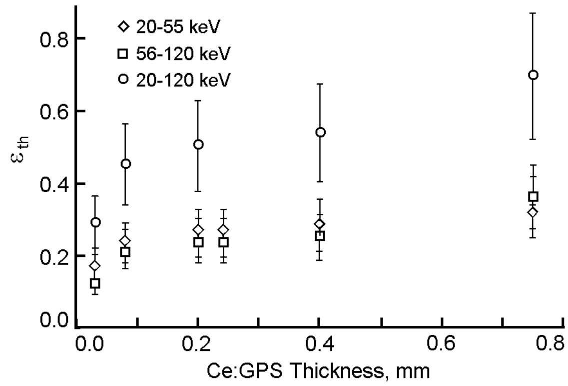


Fig. 17. The $\varepsilon_{th}$-values for the combined detectors (the reference stilbene single crystal and a Ce:GPS composite scintillator with different $L_{GPS}$) those were obtained for different energy ranges of the scintillation amplitude spectrum (see Fig. 15).

20 to 55 keV (the range of the scintillation peak generated by 33 keV conversion electrons), from 56 to 120 keV (the range of total 77 keV peak), and from 20 to 120 keV [9].

Fig. 17 shows the results of the same estimation of the efficiency of thermal neutron detection $\varepsilon_{th}$ for an other type of the combined detector. In these measurements instead of the composite stilbene detector we used the reference stilbene single crystal. We run the measurements for 5 different composite scintillators containing Ce:GPS grains with $L_{GPS}$ in the following ranges: less than 0.06, from 0.06 to 0.1, from 0.1 to 0.3, from 0.3 to 0.5 and from 0.5 to 1 mm. If we do not take into account the result obtained for the composite scintillator that contains Ce:GPS grains with $L_{GPS}$ < 0.06 mm (see Fig. 17), then the rest of the $\varepsilon_{th}$-values are in a good agreement both with $\varepsilon_{th}$-values presented by Fig. 16 and with the $\varepsilon_{th}$-values obtained earlier (see e.g. [9]). In the fraction of grains with $L_{GPS}$ < 0.06 mm there are a lot of grains with sizes too small for effective detection even of 33 keV secondary electrons. Therefore the $\varepsilon_{th}$-value of such a scintillator decreases.

The comparison of the values of scintillation amplitudes in the range that is marked by lines 1–3 on Fig. 15 and in the range of the neutron spectrum (see Fig. 14) shows that the signals from thermal and fast neutrons do not overlap. So, the analysis of these two spectra can be carried our in different energy windows.

## *5. Conclusions*

The technology of organic composite scintillators as fast neutron detectors as well as inorganic composite scintillators as detectors of thermal neutrons was discussed. For stilbene composite scintillators, the fast neutron detection efficiency is about 50–55 % with respect to organic single crystals of the same size. The single-layer composite scintillators with the Ce:GSO or Ce:GPS crystal grain size less than 0.1 mm provides detection of thermal neutrons by registration of scintillation pulses of 33 keV conversion electrons (the energy range 20 to 55 keV) with efficiency $\varepsilon_{th}$ ~ 20 %. At simultaneous registration of scintillation pulses of conversion electrons (33 keV) and the total signal (77 keV), the $\varepsilon_{th}$-values is from 40 to 50 % in the range from 20 to 120 keV.

Scintillation signals obtained from thermal and fast neutrons can be detected by the combined composite detector in different ranges of light intensities (from $10^2$ to $10^3$ photons and about $10^4$ photons, respectively). The electronics linear over a wide dynamic range will be necessary to use with such a detector. Nevertheless the signals from fast and thermal neutrons could be analyzed in two different bands of amplitudes separately. It simplifies the task.

We made our experiments for low background gamma radiation and low fluxes of neutrons. For higher intensities of gamma radiation a witness detector or combination of witness detector and shielding is necessary. The selective detection of thermal neutrons in the presence of background gamma radiation is an important problem and merits careful consideration for each concrete case.

The composite and combined composite scintillation detectors we proposed are non-hygroscopic, effective detectors of thermal and fast neutrons. They have no technological limitation on theirs shape and on the area of theirs input window.

### *References*


1. The 2007 Recommendations of the International Commission on Radiological Protection. Publication 103, *Annals of the ICRP*, **37**, 1 (2007).
2. L.Reeder, *Nucl.Instr.and Meth. Phys. Rev. A.*, **340**, 371 (1994).
3. J.Haruna, J.H.Kaneko, M.Higuchi et al., in: Conference Record of 2007 IEEE Nuclear Science Symposium and Medical Image Conference, Hawaii, USA (2008), p.1421.
4. S.V.Budakovsky, N.Z.Galunov, B.V.Grinyov et al., *Radiat.Meas.*, **42**, 565 (2007).
5. N.L.Karavaeva, O.A.Tarasenko, *Functional Materials*, **16**, 92 (2009).
6. Uk. Pat. 37010, 2008.
7. Ukr. Pat. 86136, 2009.
8. O.Sidletskiy, V.Baumer, V.Bondar et al., *Radiat.Meas.*, **45**, 365 (2010).
9. N.Z.Galunov, B.V.Grinyov, N.L.Karavaeva et al., *IEEE Trans.Nucl.Sc.*, **58**, 339 (2011).
10. Ukr.Pat. 94678,2011.
11. N.Z.Galunov, B.V.Grinyov, N.L.Karavaeva et al., *IEEE Trans.Nucl.Sci.*, **56**, 904 (2009).
12. S.K.Lee, Y.H.Cho, B.H.Kang et al., *Progress in Nucl. Scie.. Technol.*, **1**, 292 (2011).
13. J.Iwanowska, L.Swiderski, M.Moszynski et al., *J. Instrum.*, **6**, 1 (2011).
14. Photomultipliers, Ruislip, UK: Electron Tubes Enterprises Limited (2007).
15. J.H.Baker, N.Z.Galunov, A.M.Stepanenko, O.A.Tarasenko, *Radiat.Meas.*, **38**, 817 (2004).
16. S.V.Budakovsky, N.Z.Galunov, N.L.Karavaeva et al., *IEEE Trans.Nucl.Sci.*, **54**, 2734 (2007).
17. N.Z.Galunov, V.P.Seminozhenko, Teoriya i Primenenie Radioluminestsentsii Organicheskih Kondensirovannyh Sred, Naukova Dumka, Kiev (1997) [in Russian].


## Нові сцинтилятори для детектування швидких та теплових нейтронів

***М.З.Галунов, Н.Л.Караваєва, В.П.Семиноженко***

Запропоновано технологію створення нового класу детекторів — органічних композиційних сцинтиляторів. Запропонована технологія дозволяє створювати систему детектування необмеженої площини. Розглянуто воднемісткі композиційні сцинтилятори як детектори швидких нейтронів. Як детектори теплових нейтронів обговорюються композиційні сцинтилятори на основі силікату й піросилікату гадолінію. Розглядається комбінований детектор для селективної реєстрації теплових і швидких нейтронів у присутності фонового гамма-випромінювання. Сцинтиляційні характеристики композиційних детекторів аналізуються у порівнянні із традиційними монокристалічними системами.